Am J Transl Res 2018;10(8):2277-2289
www.ajtr.org /ISSN:1943-8141/AJTR0072291

Original Article

Diagnostic utility of fluorogenic peptide-conjugated Au nanoparticle probe corroborated by rabbit model of mild cartilage injury and panel of osteoarthritic patients

Zhenlong Liu[1,2], Xiaoqing Hu[2], Peng Yang[2], Jiying Zhang[2], Chunyan Zhou[1], Yingfang Ao[2]

[1]*Department of Biochemistry and Molecular Biology, School of Basic Medical Sciences, Key Laboratory of Molecular Cardiovascular Sciences (Ministry of Education), Peking University, Beijing 100191, China;* [2]*Institute of Sports Medicine, Peking University Third Hospital, Beijing Key Laboratory of Sports Injuries, Beijing 100191, China*

Received January 8, 2018; Accepted June 18, 2018; Epub August 15, 2018; Published August 30, 2018

Abstract: Using a rabbit model of early-stage osteoarthritis (OA) and a sampling patients with OA, we evaluated the diagnostic utility of a fluorogenic peptide-conjugated gold nanoparticle (AuNP) probe in detecting mild cartilage injury, based on the a disintegrin and metalloproteinase with thrombospondin motifs 4 (ADAMTS-4) enzyme. Synthesis of this fluorescent turn-on probe (or AU-probe) required conjugation of AuNPs with a fluorescein isothiocyanate (FITC)-modified ADAMTS-4-specific peptide (DVQEFRGVTAVIR). Synovial fluid samples were then collected from 48 adult rabbits and 100 patients for comparative testing (ADAMTS-4 ELISA and AU-probe). Rabbit and patient MRI images were also evaluated and scored. Receiver operating characteristic (ROC) curve analysis was applied to various diagnostic methods (MRI, ELISA, AU-probe, and arthroscopy), performing comparisons via logistic regression. In rabbits, the AU-probe proved nonsuperior to MRI T2 mapping and ELISA (fluorescence cutpoint > 864.965 au). In patient groups, logistic regression analysis indicated that combined AU-probe/MRI testing outperformed MRI alone, thus offsetting low MRI sensitivity and low AU-probe specificity for improved detection of mild cartilage injury (sensitivity, 82.5%; specificity, 80.0%). We have consequently confirmed the efficacy of this AU-probe, using ADAMTS-4 activity in synovial fluid to diagnose mild cartilage injury. Combining the AU-probe with conventional MRI assessment proved optimal in this setting.

Keywords: ADAMTS-4, gold nanoparticle probe, cartilage injury

Introduction

Osteoarthritis (OA) is one of the most common joint disorders, marked by degradation of cartilage and bony remodeling [1, 2]. Typically, it is diagnosed at an advanced stage and cannot be prevented or cured as yet. The degradation of cartilage that takes place at the onset of OA is completely reversible only if the degree of injury is mild [3, 4], which is rarely the case in routine practice. The MRI studies (T1, T2, PD series) customarily performed to evaluate joint cartilage lack the sensitivity to discern mild injury [5]. Although T2 mapping and T1-RHO series are more sensitive in this regard, such tests are time-consuming and device dependent, limiting their application to basic research [6, 7]. Screening of biomarkers associated with injured cartilage by enzyme-linked immunosorbent assay (ELISA) and western blotting is likewise reserved for research purposes, given inherent complexities and time requirements [8]. In this setting, a simple, inexpensive method of diagnosing mild cartilage injury would be ideal.

A disintegrin and metalloproteinase with thrombospondin motif-4 (ADAMTS-4) is an enzyme pivotal in the degradation of aggrecan, which occurs early in cartilage-degrading joint diseases [9, 10]. The aggrecan interglobular domain (IGD) is also cleaved at the Glu373-Ala374 bond [11]. Following the loss of aggrecan, collagen fibrils are degraded, and irreversible tissue failure ensues [12]. A means of gauging ADAMTS-4 activity could thus be useful clinically, enabling early detection of joint degeneration and disease-modifying therapeutic intervention. An

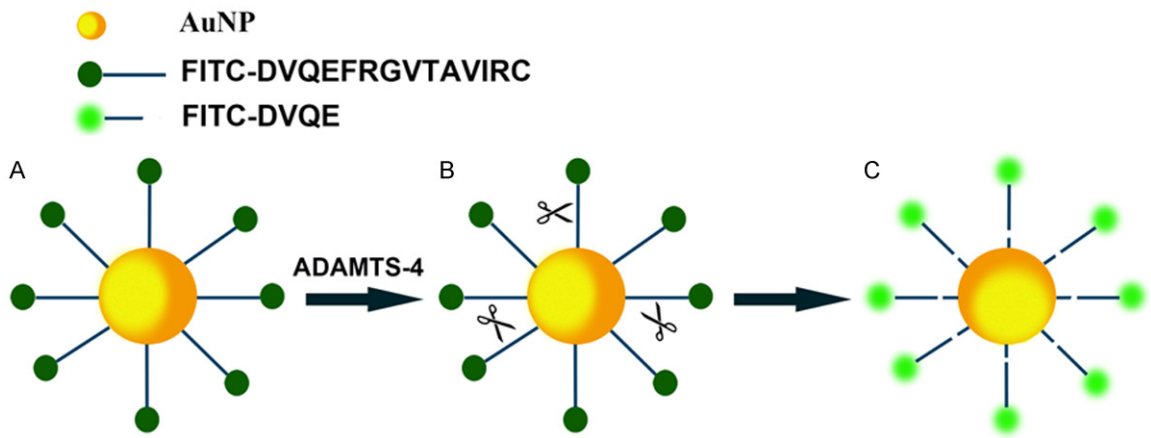

Schematic 1. Rationale of AU-probe for detection of ADAMTS-4: (A) AuNPs may quench FITC-peptide fluorescence when bonding occurs; (B) For 1 hour, AU-probe reacted with ADAMTS-4; and (C) ADAMTS-4 cleaves aggrecan at E-F bond, with restoration of FITC fluorescence as FITC and AuNPs further separate.

Table 1. Patient characteristics

Parameters	Group 0 (n = 20)	Group 1 (n = 20)	Group 2 (n = 20)	Group 3 (n = 20)	Group 4 (n = 20)	*P* value
Male/female	10/10	13/7	12/8	11/9	11/9	n.s
Age (range)	28.3 (18-47)	29.3 (19-49)	30.1 (20-51)	27.9 (19-50)	28.58 (19-47)	n.s

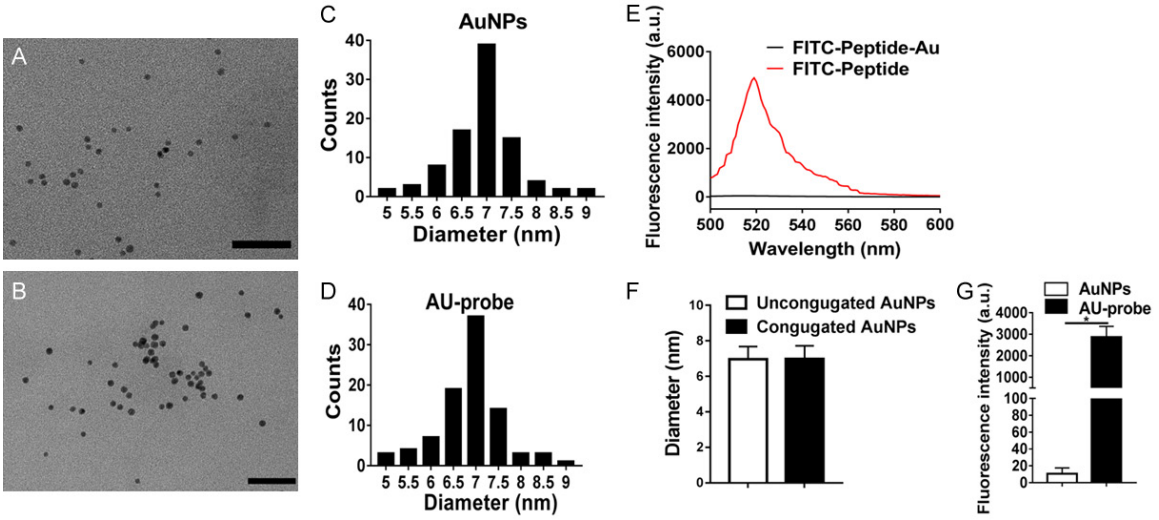

Figure 1. Characteristics of AuNPs and AU-probe: (A) TEM images of unconjugated AuNPs (scale bar, 50 nm); (B) TEM images of conjugated AuNPs (scale bar, 50 nm); (C) Distribution of unconjugated AuNPs diameters; (D) Distribution of conjugated AuNPs diameters; (E) Fluorescence intensity curve of AuNP/FITC-peptide conjugate and FITC-peptide only; (F) Statistical comparison of conjugated and unconjugated AuNP diameters; and (G) Fluorescence intensity of AU-probe and AuNPs reacting with pure recombinant ADAMTS-4, respectively.

ADAMTS-4-specific 13-mer peptide, DVQEFRGVTAVIR (Asp-Val-Gln-Glu-Phe-Arg-Gly-Val-Thr-Ala-Val-Ile-Arg) has been screened previously.

Gold nanoparticles (AuNPs) have special optical properties, including high extinction coefficients and localized surface plasmon resonance (LSPR). Such properties promote the quenching of fluorescence upon exposing fluorescein isothiocyanate (FITC) to AuNPs [13], although fluorescence is restored as FITC and AuNPs are again separated. Moreover, the surfaces of AuNPs are easily modified through strong covalent bonds or physical adsorption based on chemical characteristics. Various studies have reported that the surfaces of

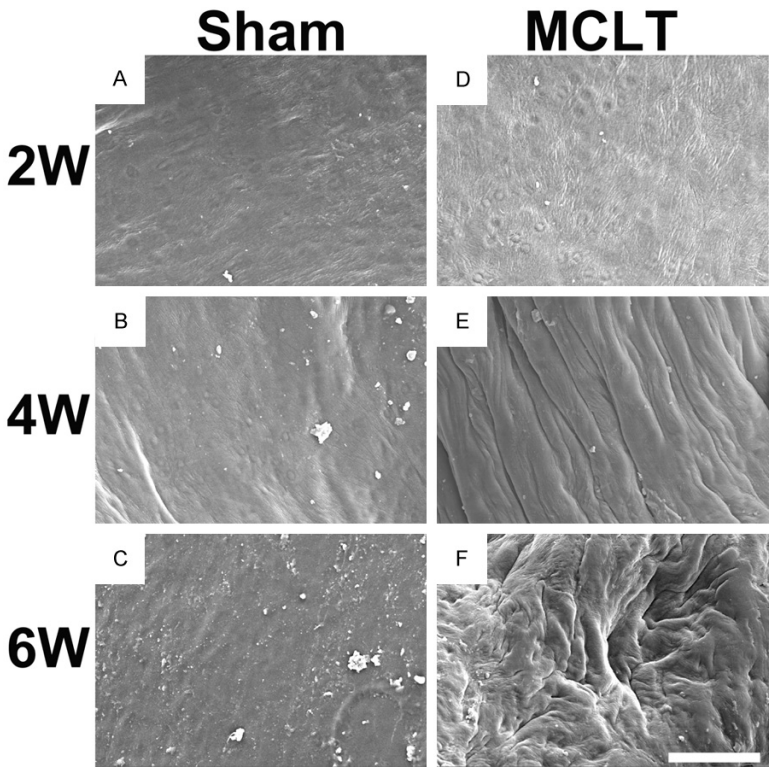

Figure 2. Evaluation of medial condylar articular cartilage at 2, 4, and 6 weeks postoperatively by scanning electron microscopy: No obvious changes in surface cartilage of sham group (A-C). In MCLT group (D-F), uneven and slightly rough surfaces observed at 4 weeks. Surface cartilage appears rougher at 6 weeks (n = 3; scale bar, 100 μm).

AuNPs may be modified accordingly, using FITC-molecules of proteins or nucleic acid to detect ions, small molecules, and enzymes [14, 15]. Reactive cysteine sulfhydryl groups readily bond to the surfaces of AuNPs, thereby serving as the basis of our research.

In an earlier work, we developed an ADAMTS-4 detective fluorescent turn-on AuNP probe (AU-probe) by conjugating gold nanoparticles with a FITC-modified ADAMTS-4-specific peptide (DVQEFRGVTAVIRC) (**Schematic 1**) [16]. The present effort was undertaken to establish the diagnostic utility of this AU-probe in osteoarthritic patients and in a rabbit model of mild cartilage injury.

Materials and methods

Preparation of AuNPs and AuNP/FITC-DVQEFRGVTAVIRC conjugate (AU-probe)

AuNPs were synthesized by reduction of $HAuCl_4 \cdot 3H_2O$ (Aladdin Reagent Inc, Shanghai, China), adding 1.0% $HAuCl_4$ (0.5 mL) to a reaction flask containing deionized water (47 mL) and heating to 60°C. A mixture of 1% sodium citrate (2 mL; Sigma-Aldrich, St Louis, MO, USA) and 1.0% tannic acid (50 μL; Sigma-Aldrich) was then rapidly added, and the solution was heated to reflux, allowing the reaction to continue (1 min) under uniform and vigorous stirring. In the process, a color change occurred (light yellow → wine red). The AuNP solution was pH-adjusted (7.0) and stored (4°C). AuNP diameters and monodispersity were later examined by transmission electron microscope (Tecnai T20 TEM; FEI [Thermo Fisher], Hillsboro, OR, USA), capturing images (200 kV, 0.35 nm point-to-point resolution). Samples were prepared by pipetting nanoparticulate suspension (10 μL) onto carbon-coated copper grid and allowing the layer (5-50 nm) to settle (20 s), using absorbent tissue to wick away any residual. Image J freeware (National Institutes of Health, Bethesda, MD, USA) helped generate a distribution of nanoparticles by size.

Conjugation of FITC-peptide to AuNPs was achieved as previously reported. Purchased (GL Biochem Ltd, Shanghai, China) FITC-conjugated DVQEFRGVTA-VIRC peptide (FITC-Asp-Val-Gln-Glu-Phe-Arg-Gly-Val-Thr-Ala-Val-Ile-Arg-Cys) in solution (1.0 mL; 1.0 mg/mL deionized water) was added dropwise to AuNP solution (10 mL, room temperature) under vigorous stirring for sustained (24 h) reaction. Resultant particles were then washed (three times) with deionized water and stored (4°C). Fluorescence intensity before and after conjugation was assessed using an automatic microplate reader (Thermo Fisher Scientific, Waltham, MA, USA). To gauge conjugate availability, the AU-probe (60 μM) was then reacted with 5 pm pure recombinant ADAMTS-4 (AnaSpec, Fremont, CA, USA) in reaction buffer (50 mM Tris·HCl, 5 mM $CaCl_2 \cdot 2H_2O$, 150 mM NaCl, pH 7.5; 100 μL total volume, 37°C, 1 h),

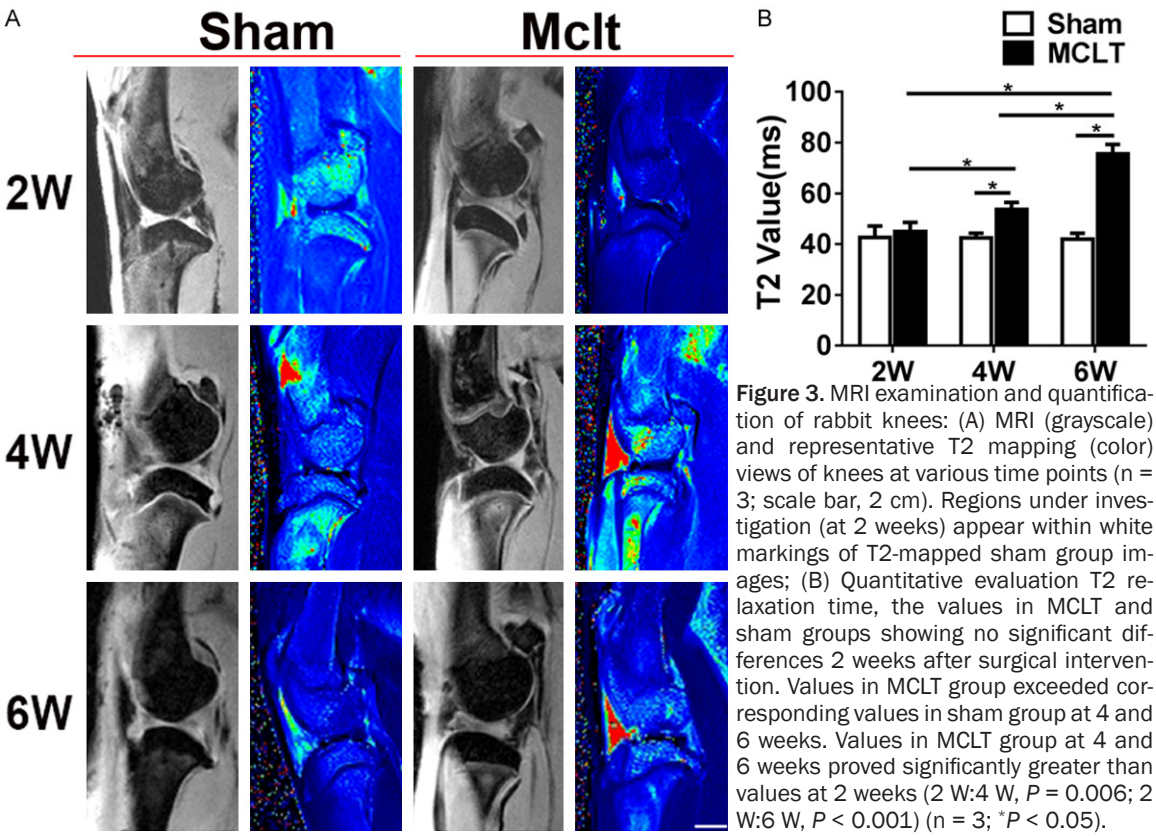

Figure 3. MRI examination and quantification of rabbit knees: (A) MRI (grayscale) and representative T2 mapping (color) views of knees at various time points (n = 3; scale bar, 2 cm). Regions under investigation (at 2 weeks) appear within white markings of T2-mapped sham group images; (B) Quantitative evaluation T2 relaxation time, the values in MCLT and sham groups showing no significant differences 2 weeks after surgical intervention. Values in MCLT group exceeded corresponding values in sham group at 4 and 6 weeks. Values in MCLT group at 4 and 6 weeks proved significantly greater than values at 2 weeks (2 W:4 W, $P = 0.006$; 2 W:6 W, $P < 0.001$) (n = 3; $^{*}P < 0.05$).

recording fluorescence data by automatic microplate reader (Thermo Fisher) once the reaction stopped. AuNPs reacted with 5 pm pure recombinant ADAMTS-4 served as control.

Cartilage-injury rabbit model

New Zealand white rabbits (N = 48) aged 4-6 months and weighing 2.5-3.0 kg were procured for this investigation. To create our model of mild cartilage degeneration (for tissue and synovial fluid analysis), we performed medial collateral ligament transection (MCLT) beyond the capsule. Each procedure was conducted as previously described [17], assigning the knees of rabbits to either MCLT (left-sided) or sham (right-sided) groups. Sham procedures were limited to skin incisions (no MCLTs). Eight knees in each group were harvested 2, 4 and 6 weeks later.

High-resolution field emission scanning electron microscope (FESEM) was used to assess microscopic changes of articular cartilage in damaged areas (n = 3). Joint samples (n = 8) were similarly evaluated through MRI studies, including T2 mapping. Mid-medial condyles (n = 8) were also serially sectioned (5 μm) in sagittal plane for histologic processing, staining slide preparations routinely (hematoxylin/eosin [HE]) and selectively (toluidine blue). To assess changes in collagen (types I and II), immunohistochemical staining took place (n = 8). At postoperative Weeks 2, 4 and 6, a normal saline wash (1500 μL) was injected into knee capsules just prior to harvesting. The fluid was then aspirated via sterile knee puncture, removing cells by centrifugation. All samples were stored (-80°C) for later investigation (ELISA and AU-probe).

Patient information and synovial fluid sampling

A total of 100 patients undergoing knee surgery (for meniscus repair, with/without cartilage degeneration) qualified for study (**Table 1**). Informed consent was obtained in each instance, as stipulated by the ethical review committee of Peking University Third Hospital. Conventional MRI (T1, T2, PD) views of the knee were examined by experienced radiologists and surgeons to assess knee cartilage preoperatively. The Outerbridge classification system was applied to grade MRI (T2) findings as follows: grade 0, intact cartilage; grade 1, signal

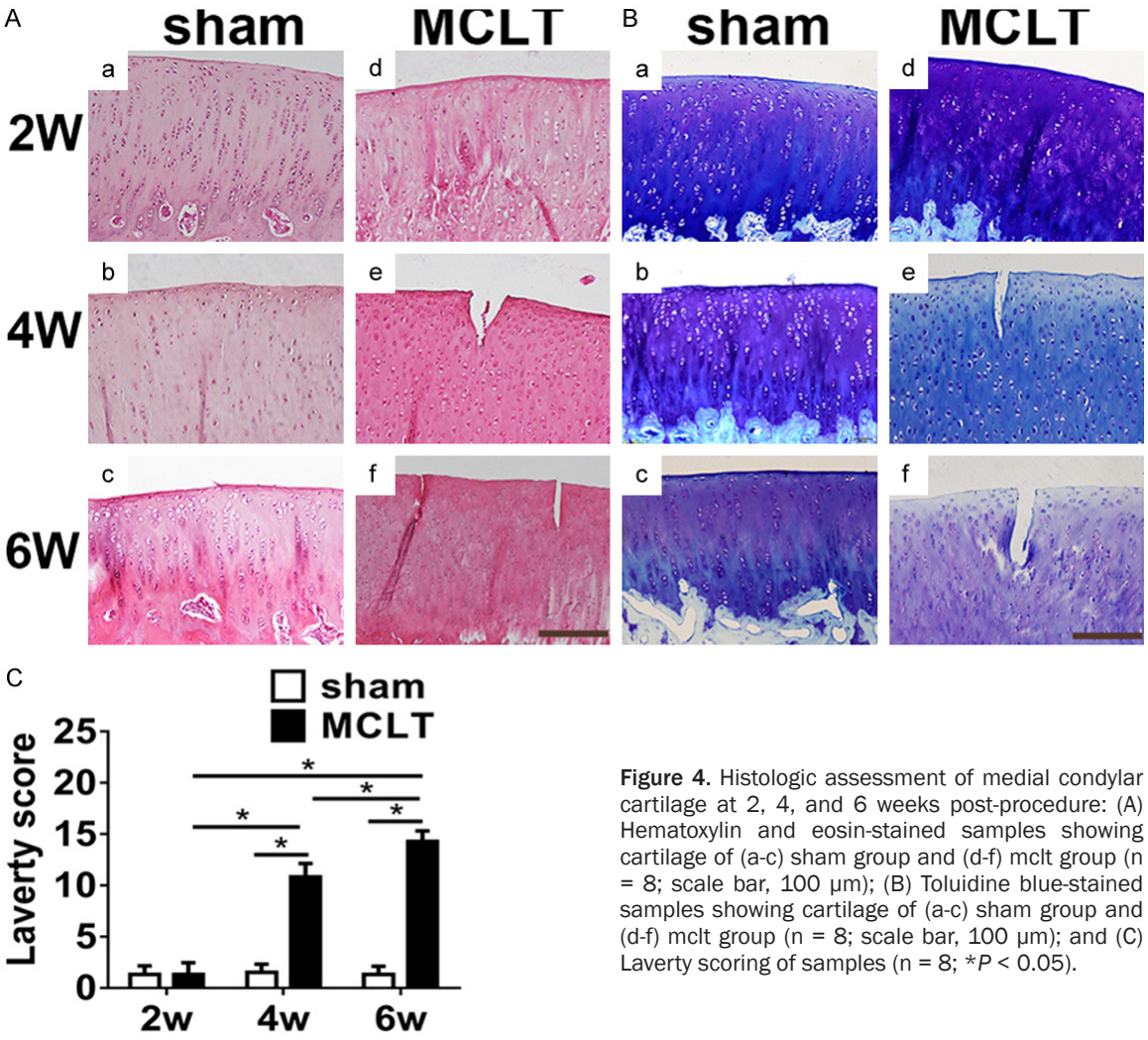

Figure 4. Histologic assessment of medial condylar cartilage at 2, 4, and 6 weeks post-procedure: (A) Hematoxylin and eosin-stained samples showing cartilage of (a-c) sham group and (d-f) mclt group (n = 8; scale bar, 100 μm); (B) Toluidine blue-stained samples showing cartilage of (a-c) sham group and (d-f) mclt group (n = 8; scale bar, 100 μm); and (C) Laverty scoring of samples (n = 8; *$P < 0.05$).

change on T2-weighted MR images; grade 2, defect of cartilage < 50% deep; grade 3, defect of cartilage > 50% deep; and grade 4, full-thickness defect of cartilage with exposed subchondral bone. Highest grades prevailed in instances of multifocal defects. Arthroscopic evaluation was still considered the "gold standard" for assessing deteriorated knee cartilage, again invoking the 5-point Outerbridge scale [18] as follows: grade 0, normal articular cartilage; grade 1, softening or blistering of joint cartilage; grade 2, cartilage fragmentation or surface fissures < 1 cm across; grade 3, cartilage fragmentation/fissuring > 1 cm across; and grade 4, eroded cartilage exposing subchondral bone. The most severe of several injured regions was graded by default.

Patients were ultimately stratified (n = 20 each subset) using the following arthroscopically determined Outerbridge grades: group 0, injured meniscus only (no cartilage defects); group 1, injured meniscus + cartilage (grade 1); group 2, injured meniscus + cartilage (grade 2); injured meniscus + cartilage (grade 3); and group 4, injured meniscus + cartilage (grade 4). Synovial fluid harvested from each group following physiologic saline (20 ml) joint injections were stored (-80°C) in aliquots (100 μL) for subsequent use, limited to one freeze-thaw event only. All procedures were approved by the ethical review committee of Peking University Third Hospital (number IRB00006761-2010085).

Screening of ADAMTS-4 activity in rabbit and human synovial fluid using probe

Diluted synovial fluid was incubated with AU-probe (60 μM; 100 μL total volume, 37°C, 1 h). Each sample (100 μL) was then diluted (500 μL) for fluorescence testing. Three synovial fluid aliquots per rabbit or patient were assay-

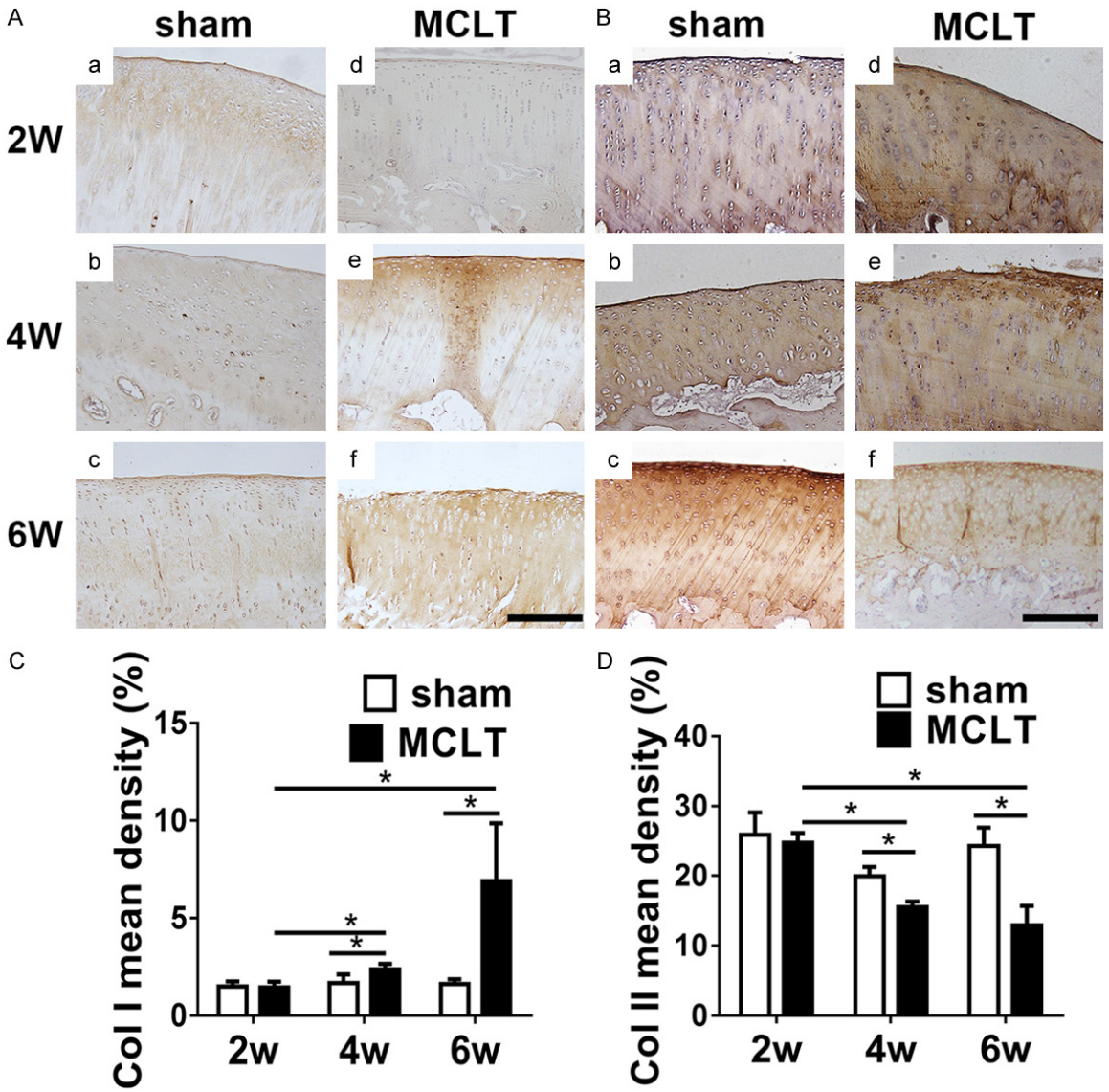

Figure 5. Immunohistochemical staining of collagen (types I and II) in medial condylar cartilage at 2, 4, and 6 weeks post-procedure: (A) Type I collagen changes shown in (a-c) sham group and (d-f) MCLT group (n = 8; scale bar, 200 μm); (B) Type II collagen changes shown in (a-c) sham group and (d-f) MCLT group (n = 8; scale bar, 200 μm); (C) Mean density of collagen type I in MCLT group exceeded that of sham group at 4 and 6 weeks (4 W, $P = 0.018$; 6 W, $P = 0.004$); and (D) Mean density of collagen type II in MCLT group exceeded that of sham group at 4 and 6 weeks (4 W, $P < 0.001$; 6 W, $P < 0.001$).

ed, expressing results as mean ± standard deviation.

Enzyme-linked immunosorbent assay (ELISA) of ADAMTS-4 in synovial fluid of rabbits and patients

Levels of ADAMTS-4 in diluted synovial fluid were determined (ELISA kit; Cloud-Clone Corp, Wuhan City, China) per manufacturer's instructions, expressing results as mean ± standard deviation.

Statistical analysis

The receiver operating characteristic (ROC) curve, area under the curve (AUC), and Youden index were used to gauge accuracy, sensitivity, and specificity of various diagnostic methods. AUC was expressed as mean ± standard error, all other data indicative of mean ± standard deviation. One-way analysis of variance (ANOVA) served to compare patient groups and animal MCLT subsets, assessing differences in sham and MCLT-treated rabbits by independent sam-

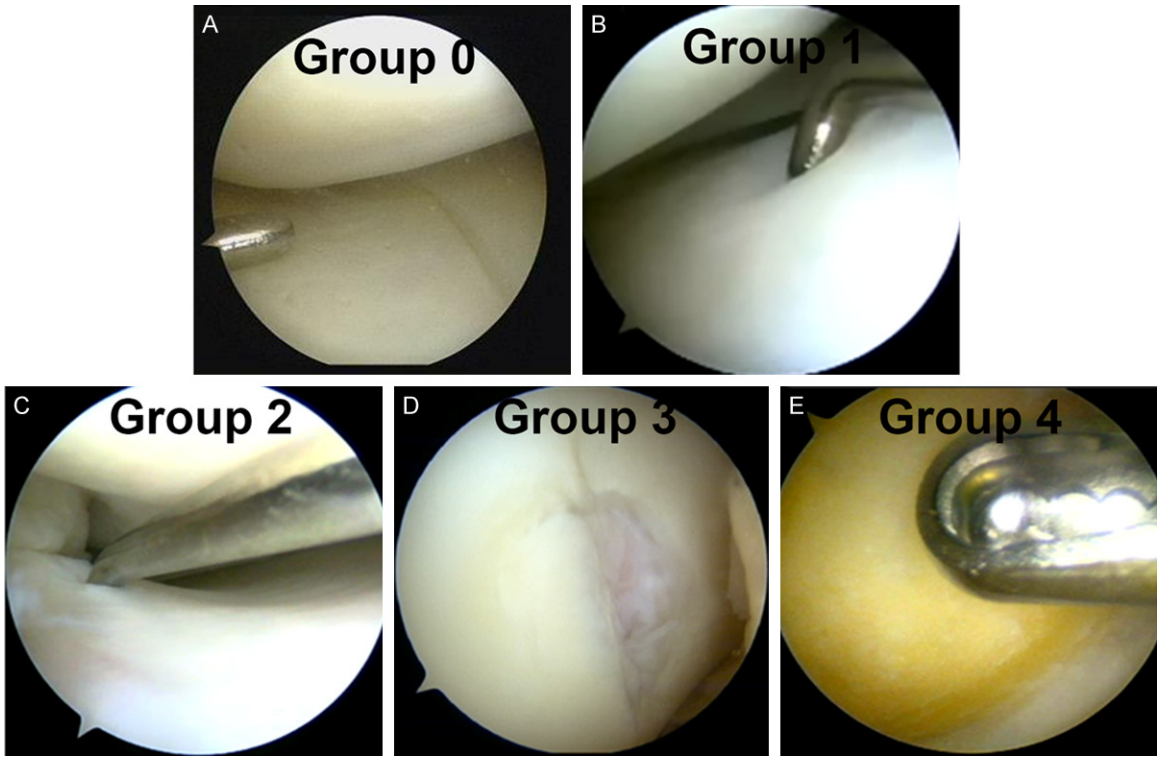

Figure 6. Arthroscopic views of cartilage injury graded by Outerbridge classification (n = 20 per group): (A) Grade 0 (normal cartilage); (B) Grade 1 (softening or blistering); (C) Grade 2 (fragmentation or fissuring of surface, < 1 cm across); (D) Grade 3 (fragmentation or fissuring > 1 cm across); and (E) Grade 4 (cartilage eroded, exposing subchondral bone).

ples *t*-test. Specific diagnostic methods were compared via binary logistic regression. To analyze combinations of methods, logistic regression was conducted. All computations relied on standard software (SPSS [IBM, Armonk, NY, USA] and MedCalc [MedCalc Software, Ostend, Belgium]), setting significance at $P < 0.05$.

Results

Characteristics of Au nanoparticles (AuNPs) and AuNP/FITC-DVQEFRGVTAVIRC conjugate (AU-probe)

As noted by TEM, unconjugated AuNPs (mean diameter, 6.96 ± 0.72 nm) were chiefly monodispersed at diameters of ~7 ± 0.5 nm. The AU-probe (FITC-peptide conjugated) remained monodispersed (mean AuNP diameter, 6.99 ± 0.73 nm), showing no significant difference in terms of unconjugated AuNPs. Dispersion of unconjugated AuNP diameters was largely stable at ~7 ± 0.5 nm. Peak fluorescence of the AuNP/FITC-peptide conjugate (AU-probe, 41.25 ± 5.7 au) was vastly weaker than that of FITC-peptide alone (4761.89 ± 358.7 au; $P < 0.001$). However, the fluorescence observed upon AU-probe reactivity with pure recombinant ADAMTS-4 (2871 ± 176.1 au) proved significantly more intense than that of ADAMTS-4 reacting solely with AuNPs (10.5 ± 2.49 au; $P < 0.001$) (**Figure 1**).

Evaluating injury to articular cartilage of rabbits (ultrastructural, MRI, and histologic manifestations)

Ultrastructural changes of articular cartilage were documented postoperatively via SEM. In the sham group, surface cartilage was uniform and smooth throughout the experimental period. By comparison, slight surface unevenness appeared in the MCLT group 4 weeks after surgery, progressing to overtly rough surfaces at 6 weeks in the absence of any fissures (**Figure 2**).

Conventional MRI and T2-mapping images were both used to evaluate injury of cartilage, which was unapparent by conventional means in both MCLT and sham groups. At 4 and 6 weeks, quantitative changes in T2-mapping images were significantly greater in the MCLT group than in the sham group; and T2-mapping values of the MCLT group at 4 and 6 weeks

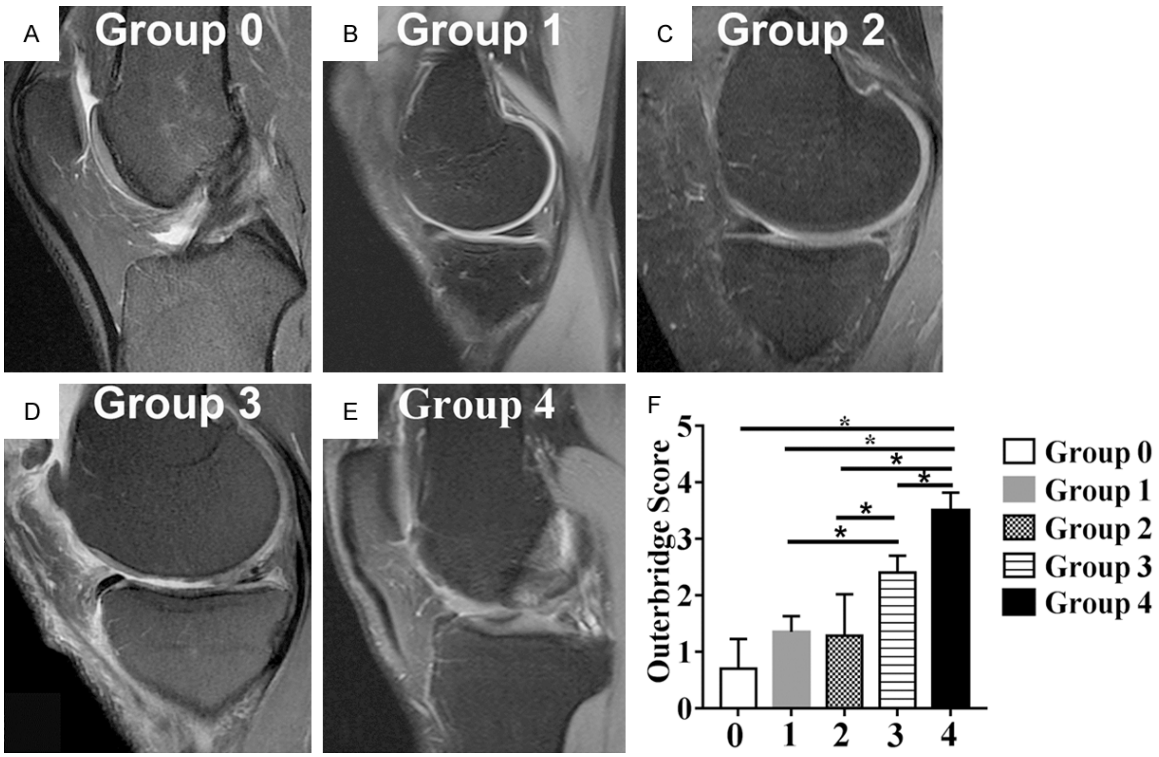

Figure 7. T2 MRI scoring of patients by Outerbridge scale: (A) Group 0, no obvious cartilage injury; (B and C) groups 1 and 2, cartilage injury difficult to detect; (D and E) Outerbridge MRI scores of patients in groups 3 (2.4 ± 0.3) and 4 (3.5 ± 0.32) proved significantly higher than those of patients in groups 0 (0.7 ± 0.53), 1 (1.35 ± 0.28), and 2 (2.4 ± 0.74) ($P < 0.001$); and (F) Outerbridge scores of MRI images.

were significantly greater than values at 2 weeks (**Figure 3**).

Histologic features of articular cartilage were examined in HE- and toluidine blue-stained sections. Throughout the experimental period, the sham group was devoid of any apparent degeneration. In the MCLT group, cartilaginous surfaces were intact at 2 weeks, with some fissures detectable at 4 weeks. These fissures increased and deepened by 6 weeks (**Figure 4A** and **4B**). Compared with the sham group, toluidine blue staining weakened at 4 and 6 weeks; and Laverty scores of the MCLT group at 4 and 6 weeks significantly surpassed scores of the sham group (4 W, $P = 0.002$; 6 W, $P < 0.001$). In the MCLT group, Laverty scores of cartilage at 4 weeks were higher than those at 2 weeks postoperatively ($P < 0.001$), and Laverty scores at 6 weeks exceeded those at 2 and 4 weeks postoperatively (6 W:2 W, $P < 0.001$; 6 W:4 W, $P < 0.001$) (**Figure 3**). Actual Laverty scores are provided in a supplementary table (Supplementary Table 1).

In the MCLT group, staining of type II collagen progressively weakened over time. Between 2 and 6 weeks, the mean density of type II collagen declined dramatically (2 W:4 W, $P < 0.001$; 2 W:6 W, $P < 0.001$; 4 W:6 W, $P = 0.081$), whereas type I collagen showed a significant increase in mean density during the same period (2 W:4 W, $P = 0.004$; 2 W:6 W, $P < 0.001$; 4 W:6 W, $P < 0.001$) (**Figure 5**).

Evaluating articular cartilage in patients (MRI and arthroscopic Outerbridge grading)

All compartments of the knee joints were evaluated via arthroscopy, assigning 20 patients with meniscus injury only to group 0; 20 patients with meniscus injury and grade 1 cartilage injury to group 1; 20 patients with meniscus injury and grade 2 cartilage injury to group 2; 20 patients with meniscus injury and grade 3 cartilage injury to group 3; and 20 patients with meniscus injury and grade 4 cartilage injury to group 4 (**Figure 6**).

Outerbridge MRI scores of patients in groups 3 (2.4 ± 0.3) and 4 (3.5 ± 0.32) exceeded those of patients in groups 0 (0.7 ± 0.53), 1 (1.35 ± 0.28), and 2 (2.4 ± 0.74) to a significant degree ($P < 0.001$). In T2 MRI views, injury to cartilage

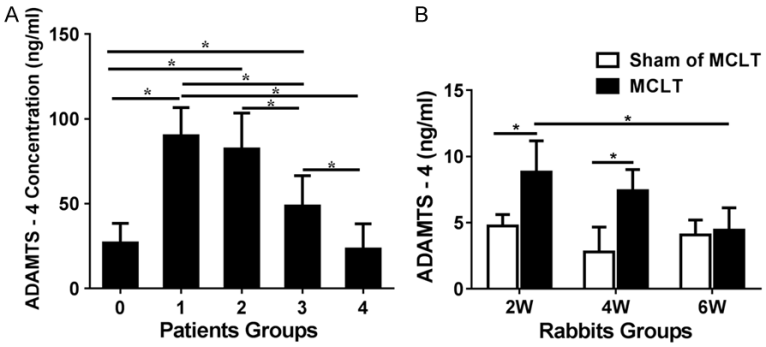

Figure 8. Results of patient and rabbit synovial fluid analysis (ADAMTS-4 ELISA): (A) Concentration of ADAMTS-4 in synovial fluid collected from patients of group 0 proved lower than levels in patients of groups 1, 2, and 3 ($P < 0.001$). Mean ADAMTS-4 concentration gradually declined in groups 1 through 4. Average ADAMTS-4 level of patients in group 2 surpassed average levels of patients in groups 3 and 4 (2:3, $P < 0.001$; 2:4, $P < 0.001$); and concentration in group 3 exceeded that of group 4 ($P < 0.001$); and (B) At 2 and 4 weeks after MCLT, ADAMTS-4 concentration dramatically increased, compared with sham group (2 w: $P = 0.006$; 4 w: $P = 0.003$). In MCLT group, synovial fluid ADAMTS-4 concentration at 2 weeks significantly exceeded that found at 6 weeks ($P = 0.004$). No significant difference in ADAMTS-4 concentrations of MCLT and sham groups at 6 weeks postoperatively.

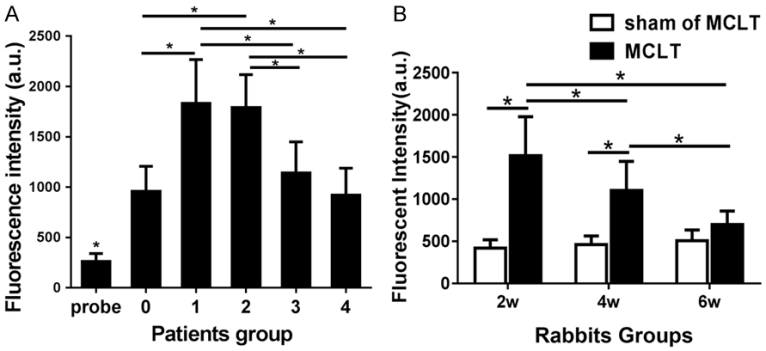

Figure 9. Results of patient and rabbit synovial fluid analysis (AU-probe): (A) Fluorescence recovery, nearly undetectable in probe control group, figured prominently in patients of groups 1 and 2, compared with those of group 0 (1:0, $P < 0.001$; 2:0, $P < 0.001$). Fluorescence recovery in patient groups 3 and 4 proved weaker than that encountered in groups 1 and 2 (1:3, $P < 0.001$; 1:4, $P < 0.001$; 2:3, $P < 0.001$; 2:4, $P < 0.001$). Patients in groups 3 and 4 did not differ significantly; and (B) Fluorescence recovery in rabbit synovial fluid collected at 2 and 4 weeks tested significantly higher for MCLT group, compared with sham group (2 weeks, $P < 0.001$; 4 weeks, $P < 0.001$). Synovial fluid samples collected at 2 and 4 weeks showed decisively higher recovery than samples collected from rabbits at 6 weeks (2 W:6 W, $P = 0.006$; 4 W:6 W, $P = 0.046$).

was not evident in patients of group 0 and was difficult to detect in patients of groups 1 and 2 (**Figure 7**).

Detection of ADAMTS-4 activity (ELISA) in synovial fluid of rabbits

At 2 and 4 weeks after MCLT, the concentration of ADAMTS-4 in synovial fluid showed dramatic increases, compared with levels in the sham group (2 W, $P = 0.006$; 4 W, $P = 0.003$). In the MCLT group, the ADAMTS-4 concentration in synovial fluid collected at 2 weeks was significantly higher than that collected at 6 weeks ($P = 0.004$) (**Figure 8B**).

Detection of ADAMTS-4 activity (ELISA) in synovial fluid of patients

ADAMTS-4 concentration in synovial fluid collected from patients of group 0 was less than corresponding levels in groups 1 through 4 ($P < 0.001$, **Figure 8A**). Overall, the mean ADAMTS-4 concentration in synovial fluid was highest in group 1, declining gradually from group 2 to group 4. Its level in group 2 exceeded levels of groups 3 and 4 (2:3, $P < 0.001$; 2:4, $P < 0.001$), and the level in group 3 exceeded that of group 4 ($P < 0.001$) (**Figure 8A**).

Detection of ADAMTS-4 activity (AU-probe) in synovial fluid of rabbits

In the MCLT group, fluorescence recovery of synovial fluid collected at 2 and 4 weeks was significantly higher than in corresponding samples of the sham group (2 W, $P < 0.001$; 4 W, $P < 0.001$). Recovery seen at 2 and 4 weeks clearly exceeded that detected at 6 weeks in rabbits (2 W:6 W, $P = 0.006$; 4 W:6 W, $P = 0.046$) (**Figure 9B**).

Detection of ADAMTS-4 activity (AU-probe) in synovial fluid of patients

Fluorescence recovery was nearly undetectable in the control group (pure probe) but was clearly observed in patients of groups 1 and 2, when compared with those of group 0 (1:0, $P < 0.001$; 2:0, $P < 0.001$). Although fluorescence recovery in groups 3 and 4 was less than that

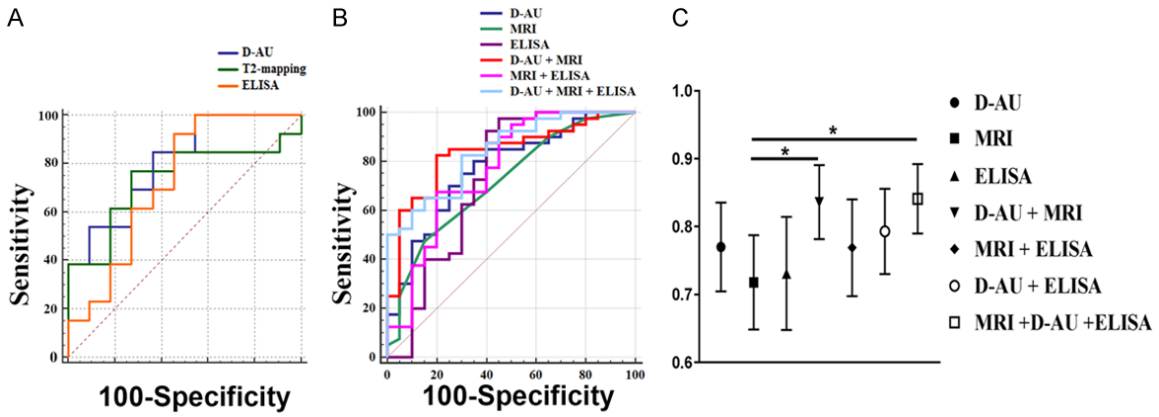

Figure 10. Results of ROC curve analysis, comparing various diagnostic methods: (A) ROC curves plotted for AU-probe, MRI T2 mapping, and ELISA applied to rabbit model; (B) ROC curves plotted for AU-probe, MRI, ELISA, and combined variables (AU-probe + MRI, MRI + ELISA, and AU-probe + MRI + ELISA); and (C) AUC determinations for AU-probe, MRI, ELISA, and combined variables (AU-probe + MRI, MRI + ELISA, AU-probe + ELISA, and AU-probe + MRI + ELISA. Both AU-probe and MRI in combination significantly outperformed MRI alone (AUC = 0.836, 95% CI: 0.541-0.959; *P* = 0.035), conferring a sensitivity of 82.5% and specificity of 80.0%. AU-probe, MRI, and ELISA in combination also performed significantly better than MRI alone (AUC = 0.841, 95% CI: 0.724-0.923; *P* = 0.455).

Table 2. Receiver operating characteristic (ROC) curve analysis of various test methods applied to rabbit samples

RABBIT	AUC	SE	95% CI	Sensitivity	Specificity	Youden Index	Cutpoint
D-AU	0.80	0.09	0.59 to 0.94	84.62	63.64	0.48	> 864.97
T2-mapping	0.73	0.11	0.52 to 0.89	76.9	72.7	0.50	> 50.1
ELISA	0.73	0.11	0.51 to 0.89	92.31	54.55	0.47	> 5.05

AUC, area under the curve; CI, confidence interval; ELISA, enzyme-linked immunosorbent assay; SE, standard error.

Table 3. Receiver operating characteristic (ROC) curve analysis of various test methods applied to patient samples

	AUC	SE	95% CI	Sensitivity	Specificity	Youden Index
D-AU	0.77	0.065	0.64 to 0.87	80	65	0.45
MRI	0.718	0.069	0.59 to 0.83	47.5	85	0.33
ELISA	0.731	0.083	0.60to 0.84	97.5	55	0.53
D-AU + MRI	0.836	0.055	0.72 to 0.92	82.5	80	0.63
D-AU + ELISA	0.793	0.063	0.67 to 0.89	77.5	70	0.48
MRI + ELISA	0.769	0.071	0.22 to 0.63	67.5	80	0.48
D-AU + MRI + ELISA	0.841	0.051	0.72 to 0.92	82.5	70	0.53

AUC, area under the curve; CI, confidence interval; ELISA, enzyme-linked immunosorbent assay; MRI, magnetic resonance imaging; SE, standard error.

of groups 1 and 2 (1:3, $P < 0.001$; 1:4, $P < 0.001$; 2:3, $P < 0.001$; 2:4, $P < 0.001$), groups 3 and 4 did not differ significantly (**Figure 9A**).

Accuracy of AU-probe in detecting mild cartilage injury of rabbit model

Outcomes of the AU-probe (AUC = 0.804, 95% CI: 0.59-0.94) did not differ significantly from those of T2 mapping (AUC = 0.73, 95% CI: 0. 0.52-0.89; Youden index = 0.50) or ELISA (AUC = 0.73, 95% CI: 0.51-0.89; Youden index = 0.47). At a fluorescence intensity > 864.965 au, mild cartilage injury was detectable (sensitivity, 84.62%; specificity, 63.64%) by AU-probe (**Figure 10A**). The cutpoint for T2 mapping was at values > 50.1 (sensitivity, 76.9%; specificity, 72.7%), and an ADAMTS-4 concentration > 5.05 was the cutpoint for ELISA (sensitivity, 92.31%; specificity, 54.55%) (**Table 2**).

Accuracy of AU-probe and MRI in detecting mild cartilage injury of patients

Again, AU-probe outcomes (AUC = 0.77, 95% CI: 0.643-0.869) did not differ significantly from those of MRI (AUC = 0.718, 95% CI: 0.59-0.83;

Youden index = 0.33) or ELISA (AUC = 0.731, 95% CI: 0.60-0.84; Youden index = 0.53). A fluorescence intensity > 1360.19 au was the cutpoint for detecting mild cartilage injury (sensitivity, 80%; specificity, 65%) by AU-probe. The cutpoint for MRI was at scores > 1 (sensitivity, 47.5%; specificity, 85%), and an ADAMTS-4 concentration > 45.9 was the cutpoint for ELISA (sensitivity, 95%; specificity, 55%).

A combined approach, using both AU-probe and MRI scoring (AUC = 0.836, 95% CI: 0.541-0.959; P = 0.035) significantly outperformed MRI scoring alone, conferring sensitivity of 82.5% and specificity of 80.0% (**Figure 10** and **Table 3**).

Discussion

As shown by patient and animal diagnostics, reflecting ADAMTS-4 activity in synovial fluid, the clinical utility of a fluorescence turn-on AU-probe for detecting mild injury of knee cartilage is no longer in doubt. When combined with conventional MRI, high sensitivity (82.5%) and specificity (80.0%) are achieved.

In our rabbit model of mild cartilage injury, histologic staining helped confirm the extent of cartilage degradation in bony samples. However, use of the AU-probe in animal testing did not prove superior to T2 mapping, thus offering no apparent clinical advantage. Many studies have underscored the merit of T2 mapping in this setting by examining images of type II collagen; but the high cost and lengthy examination times are clinically prohibitive [19, 20]. The efficacy and economy of the AU-probe make it much more suitable as a clinical tool, and its diagnostic sensitivity (84.62%) surpasses that of T2 mapping.

Compared with ELISA, there are four aspects of the AU-probe having more favorable clinical implications. Although ELISA boasts comparatively higher sensitivity (92.31% vs 84.62%), its specificity (54.55%) is quite low. Furthermore, the AU-probe requires much less synovial fluid than ELISA (20 μL vs 100 μL) and is completed in ~1 hour, compared with a 4- to 6-hour time frame for ELISA. Finally, the AU-probe identifies activated ADAMTS-4, a key element in glucosamine degradation, whereas ELISA measures total ADAMTS-4 concentrations, including zymogen content of synovial fluid [16]. Some sources have reported increased mRNA expression of ADAMTS-4 in knee cartilage of patients with late-stage OA [21, 22]; yet in severely affected patients who undergo joint replacement, expression of the inactive ADAMTS-4 proenzyme has been shown to increase, without a commensurate upsurge in activation [23, 24]. Assays of activated ADAMTS-4 are thus more telling than total ADAMTS-4 concentration in depicting the dynamics of OA.

As for the patients we studied, testing of the AU-probe produced similar results. Its diagnostic utility was at least comparable to MRI in determining mild cartilage injury. Despite showing superior sensitivity (AU-probe, 80%; MRI, 47.5%), the AU-probe was lacking in specificity. Nonetheless, logistic regression analysis of combined variables has indicated that dual AU-probe/MRI use yields better diagnostic accuracy than MRI alone (AUC = 0.836, 95% CI: 0.541-0.959; P = 0.035), conferring a sensitivity of 82.5% and 80% specificity. Unfortunately, the same was not true of MRI and ELISA.

At present, a mild stage of cartilage injury (Outerbridge grades 1 and 2) affords the only chance of cure [25, 26]. The AU-probe therefore addresses an urgent need for early OA detection. Based on the specified cutpoint (> 1360.19 au), a diagnosis of mild cartilage injury is achievable in conjunction with conventional MRI studies. The AU-probe provides a means of therapeutic monitoring. Synovial fluid collected during knee surgery or at outpatient clinics may be readily tested, allowing timely adjustments in treatment in line with the status of articular cartilage.

The chief limitation of this study was that all patients showed not only cartilage injury, but also meniscus injury. The latter may equally impact ADAMTS-4 levels in synovial fluid, producing spurious results. Because it was difficult to collect synovial fluid in the absence of other disease, meniscus injury was allowed in the patients we enlisted for our research.

Acknowledgements

We wish to thank members of Peking University Health Science Center, specifically Xinrong Zhao (for assistance with TEM of the AU-probe) and Professors Yinlin Sha and Lijun Wang (for their help in Au-probe synthesis). This work was supported by grants from the National Natural Science Foundation of China (No. 81672212, 81330040) and Beijing Municipal Natural

Science Foundation (No. 7174361). All authors have read the journal's authorship agreement and policy on disclosure of potential conflicts of interest.

Disclosure of conflict of interest

None.

Address correspondence to: Chunyan Zhou, Department of Biochemistry and Molecular Biology, School of Basic Medical Sciences, Key Laboratory of Molecular Cardiovascular Sciences (Ministry of Education), Peking University, Beijing 100191, China. Tel: +86 13641169706; E-mail: chunyanzhou@bjmu.edu.cn; Yingfang Ao, Institute of Sports Medicine, Peking University Third Hospital, Beijing Key Laboratory of Sports Injuries, Beijing 100191, China. Tel: +86 13261993917; E-mail: aoyingfang@163.com

References

[1] Lee JI, Balolong E Jr, Han Y and Lee S. Stem cells for cartilage repair: what exactly were used for treatment, cultured adipose-derived stem cells or the unexpanded stromal vascular fraction? Osteoarthritis Cartilage 2016; 24: 1302-3.

[2] Osório J. Osteoarthritis: Galectin-1 damages cartilage via inflammation. Nat Rev Rheumatol 2016; 12: 132.

[3] Onuora S. Osteoarthritis: chondrocyte clock maintains cartilage tissue. Nat Rev Rheumatol 2016; 12: 71.

[4] Apte S. Anti-ADAMTS5 monoclonal antibodies: implications for aggrecanase inhibition in osteoarthritis. Biochem J 2016; 473: e1-4.

[5] Lee J, Badar F, Kahn D, Matyas J, Qu X and Xia Y. Loading-induced changes on topographical distributions of the zonal properties of osteoarthritic tibial cartilage- A study by magnetic resonance imaging at microscopic resolution. J Biomech 2015; 48: 3634-3642.

[6] Li X, Pedoia V, Kumar D, Rivoire J, Wyatt C, Lansdown D, Amano K, Okazaki N, Savic D, Koff M, Felmlee J, Williams S and Majumdar S. Cartilage T1ρ and T2 relaxation times: longitudinal reproducibility and variations using different coils, MR systems and sites. Osteoarthritis Cartilage 2015; 23: 2214-2223.

[7] Guermazi A, Alizai H, Crema M, Trattnig S, Regatte R and Roemer F. Compositional MRI techniques for evaluation of cartilage degeneration in osteoarthritis. Osteoarthr Cartil 2015; 23: 1639-1653.

[8] Burnett W, Kontulainen S, McLennan C, Hazel D, Talmo C, Hunter D, Wilson D and Johnston J. Knee osteoarthritis patients with severe nocturnal pain have altered proximal tibial subchondral bone mineral density. Osteoarthr Cartil 2015; 23: 1483-1490.

[9] Yang CY, Chanalaris A and Troeberg L. ADAMTS and ADAM metalloproteinases in osteoarthritis-looking beyond the 'usual suspects'. Osteoarthritis Cartilage 2017; 25: 1000-1009.

[10] Mobasheri A, Bay-Jensen AC, van Spil WE, Larkin J and Levesque MC. Osteoarthritis year in review 2016: biomarkers (biochemical markers). Osteoarthritis Cartilage 2017; 25: 199-208.

[11] Tortorella MD, Pratta M, Liu RQ, Austin J, Ross OH, Abbaszade I, Burn T and Arner E. Sites of aggrecan cleavage by recombinant human aggrecanase-1 (ADAMTS-4). J Biol Chem 2000; 275: 18566-18573.

[12] Tortorella M, Pratta M, Liu RQ, Abbaszade I, Ross H, Burn T and Arner E. The thrombospondin motif of aggrecanase-1 (ADAMTS-4) is critical for aggrecan substrate recognition and cleavage. J Biol Chem 2000; 275: 25791-25797.

[13] Santhoshkumar J, Rajeshkumar S and Venkat Kumar S. Phyto-assisted synthesis, characterization and applications of gold nanoparticles-a review. Biochem Biophys Rep 2017; 11: 46-57.

[14] Ong ZY, Chen S, Nabavi E, Regoutz A, Payne DJ, Elson DS, Dexter DT, Dunlop IE and Porter AE. Multi-branched gold nanoparticles with intrinsic LAT-1 targeting capabilities for selective photothermal therapy of breast cancer. ACS Appl Mater Interfaces 2017.

[15] Kwon NK, Lee TK, Kwak SK and Kim SY. Aggregation driven controllable plasmonic transition of silica-coated gold nanoparticles with temperature dependent polymer-nanoparticle interactions for potential applications in optoelectronic devices. ACS Appl Mater Interfaces 2017; 9: 39688-39698.

[16] Peng S, Zheng Q, Zhang X, Dai L, Zhu J, Pi Y, Hu X, Cheng W, Zhou C, Sha Y and Ao Y. Detection of ADAMTS-4 activity using a fluorogenic peptide-conjugated Au nanoparticle probe in human knee synovial fluid. ACS Appl Mater Interfaces 2013; 5: 6089-6096.

[17] Liu Z, Hu X, Man Z, Zhang J, Jiang Y and Ao Y. A novel rabbit model of early osteoarthritis exhibits gradual cartilage degeneration after medial collateral ligament transection outside the joint capsule. Sci Rep 2016; 6: 34423.

[18] Health Quality Ontario. Arthroscopic lavage and debridement for osteoarthritis of the knee: an evidence-based analysis. Ont Health Technol Assess Ser 2005; 5: 1-37.

[19] Verschueren J, Meuffels DE, Bron EE, Klein S, Kleinrensink GJ, Verhaar JAN, Bierma-Zeinstra

SMA, Krestin GP, Wielopolski PA, Reijman M and Oei EHG. Possibility of quantitative T2-mapping MRI of cartilage near metal in high tibial osteotomy: a human cadaver study. J Orthop Res 2018; 36: 1206-1212.

[20] Morgan P, Nissi MJ, Hughes J, Mortazavi S and Ellerman J. T2* mapping provides information that is statistically comparable to an arthroscopic evaluation of acetabular cartilage. Cartilage 2017; 1947603517719316.

[21] Bau B, Gebhard PM, Haag J, Knorr T, Bartnik E and Aigner T. Relative messenger RNA expression profiling of collagenases and aggrecanases in human articular chondrocytes in vivo and in vitro. Arthritis Rheum 2002; 46: 2648-2657.

[22] Moulharat N, Lesur C, Thomas M, Rolland-Valognes G, Pastoureau P, Anract P, De Ceuninck F and Sabatini M. Effects of transforming growth factor-beta on aggrecanase production and proteoglycan degradation by human chondrocytes in vitro. Osteoarthritis Cartilage 2004; 12: 296-305.

[23] Uchida K, Takano S, Matsumoto T, Nagura N, Inoue G, Itakura M, Miyagi M, Aikawa J, Iwase D, Minatani A, Fujimaki H and Takaso M. Transforming growth factor activating kinase 1 regulates extracellular matrix degrading enzymes and pain-related molecule expression following tumor necrosis factor-alpha stimulation of synovial cells: an in vitro study. BMC Musculoskelet Disord 2017; 18: 283.

[24] Naito S, Shiomi T, Okada A, Kimura T, Chijiiwa M, Fujita Y, Yatabe T, Komiya K, Enomoto H, Fujikawa K and Okada Y. Expression of ADAMTS4 (aggrecanase-1) in human osteoarthritic cartilage. Pathol Int 2007; 57: 703-711.

[25] Poulet B. Models to define the stages of articular cartilage degradation in osteoarthritis development. Int J Exp Pathol 2017; 98: 120-126.

[26] Shah NJ, Geiger BC, Quadir MA, Hyder MN, Krishnan Y, Grodzinsky AJ and Hammond PT. Synthetic nanoscale electrostatic particles as growth factor carriers for cartilage repair. Bioeng Transl Med 2016; 1: 347-356.

Supplementary Table 1. Descriptive statistics for Laverty score at 2, 4 and 6 weeks after sugery

Group	Safranin o-fast green	Structure	Chondrocyte density	Cluster formation	Total score
2 W sham of MCLT	0.83 ± 0.41	0.5 ± 0.55	0	0	1.33 ± 0.82
2 W MCLT	0.67 ± 0.52	0.5 ± 0.55	0.17 ± 0.41	0	1.33 ± 1.03
4 W sham of MCLT	1	0.17 ± 0.41	0.33 ± 0.52	0	1.5 ± 0.83
4 W MCLT	4.33 ± 0.52	4.33 ± 0.82	1.67 ± 0.52	0.5 ± 0.55	10.8 ± 1.33
6 W sham of MCLT	0.67 ± 0.52	0.33 ± 0.52	0.33 ± 0.52	0	1.3 ± 0.82
6 W MCLT	4.67 ± 0.82	7 ± 0.63	1.67 ± 0.52	1 ± 0.63	14.3 ± 1.03